Combustion Synthesis and Effects of Processing Parameters on Physical Properties of α-Alumina

Melissa V. Collins* and Deidre A. Hirschfeld*
New Mexico Institute of Mining and Technology, Socorro, NM, 87801

Lauren E. Shea*
Sandia National Laboratories, Albuquerque, NM 87185

ABSTRACT

Fine particle porous α-alumina has been prepared by a wet chemical method of combustion synthesis using an aqueous precursor containing aluminum nitrate (oxidizer) and carbohydrazide, an organic fuel as starting materials. The aluminum nitrate and carbohydrazide were reacted exothermically at 400-600°C. The synthesis of α-alumina (α-Al_2O_3) was used as a model for understanding the effects of processing parameters on physical properties such as surface area, average pore size, and residual carbon content. The porous powders were characterized using x-ray diffraction (XRD), scanning electron microscopy (SEM), BET surface area analysis and elemental analysis. The decomposition of the starting materials was investigated using differential thermal and thermogravimetric analyses (DTA/TGA). It has been shown that the furnace temperature, fuel/oxidizer ratio, and precursor water content can be tailored to produce powders with different physical properties.

*Member, American Ceramic Society

DISCLAIMER

DISCLAIMER

Portions of this document may be illegible in electronic image products. Images are produced from the best available original document.

1. INTRODUCTION

Combustion synthesis describes a variety of self-sustaining synthesis reactions used to produce a variety of advanced materials. Self-propagating high temperature synthesis (SHS) is a familiar type of solid phase combustion reaction.[1] In SHS, an exothermic chain reaction occurs in pelleted reactants, e.g. metallic powder. This reaction is initiated by the ignition of one end of the pellet, or the pellet is encapsulated in a highly exothermic atmosphere and heated. Non-oxide ceramics[1,2], intermetallics[3], and functionally-graded materials[3] are among the materials successfully produced using SHS techniques.

In the late 1980s, wet chemical methods for combustion synthesis were developed. These utilize the exothermic redox reaction initiated in an aqueous precursor solution of metal nitrates (oxidizers) and carbonaceous fuels (reducing agents) to instantaneously produce homogeneous, crystalline, multicomponent oxide powders and ceramic-metal composites. Combustion synthesis using metal nitrate-urea[4-9] and metal nitrate-glycine[10-13] precursors were among the earlier examples of the process. Metal nitrate-carbohydrazide combustion synthesis has also been used successfully to produce oxide ceramics[14,15] and high efficiency phosphors[16-18]. Combustion synthesis techniques yield crystalline, multicomponent, fine particle size, porous powders in a few minutes at low temperatures. Existing synthesis techniques of fine particle multicomponent oxides such as freeze or spray drying[19], co-precipitation[20-22], sol-gel[23] and spray decomposition[24] processes are time consuming and usually require high temperature annealing steps. Wet chemical combustion reactions

are typically initiated in a muffle furnace or on a hot plate at a low temperature of 350°C or more. Typical fuels used in this process should have a relatively low ignition temperature (~250°C), non-violent combustion with a moderate gas volume, and complete conversion to non-toxic gases. The fuel also acts as a complexant for the metal cations, thereby increasing their solubility and preventing preferential crystallization of the dehydrated metal nitrate[9]. When placed in the furnace, the solution of oxidizer and fuel boils, dehydrates, and decomposes. The mixture ignites vigorously after ~3 minutes. A flame is produced in one area of the decomposed reactants and propagates through the entire mixture, until all of the precursor materials are consumed. Flame duration depends on fuel content. A large volume of gases, including traces of ammonia, are generated in the combustion reaction. The nature of the gases produced depends on the type of fuel and the fuel/oxidizer ratio. The as-synthesized products are typically voluminous, foamy powders that occupy the entire volume of the reaction vessel.

There are three important temperatures in all combustion reactions: (1) ignition temperature (T_o), which represents the point where the reaction is dynamically activated without further external heat supply; (2) actual combustion flame temperature (T_c), which is the maximum temperature achieved under non-adiabatic conditions; and (3) adiabatic combustion flame temperature (T_f), which is the maximum theoretical flame temperature achieved under adiabatic conditions. Adiabatic flame temperature can be estimated for a combustion reaction using Hess' Law which is expressed as follows:

$$T_f = T_o + \frac{\Delta H_r - \Delta H_p}{c_p} \qquad (1.1)$$

where T_f is the adiabatic flame temperature, T_o is the ignition temperature, ΔH_r is the enthalpy of the reactants, ΔH_p is the enthalpy of the products, and c_p is the heat capacity at a constant pressure. The actual flame temperature, T_c can be measured using an optical pyrometer.

Calculation of the stoichiometry of metal nitrate-fuel mixtures utilizes the principles of propellant chemistry and employs the elemental stoichiometric coefficient, Φ_e. This parameter uses the total oxidizing and reducing valencies of the components, which serve as numerical coefficients for the stoichiometric balance[15,16]. When $\Phi_e = 1$ the mixture is stoichiometric and is known to release maximum energy in condensed fuel-oxidizer systems. The mixture is fuel-lean when $\Phi_e > 1$, and fuel-rich when $\Phi_e < 1$.

The oxidizer-to-fuel molar ratio required for a stoichiometric mixture is determined by summing the total oxidizing and reducing valencies in the oxidizer and dividing by the sum of the total oxidizing and reducing valencies in the fuel, as shown in equation 1.2. In these types of calculations, oxygen is considered to be the only oxidizing element; carbon, hydrogen, and metal cations are reducing elements; and nitrogen is neutral. Oxidizing elements have positive valencies and reducing elements have negative valencies.

$$\text{Oxidizer/fuel ratio} = \frac{\Sigma \text{ all oxidizing and reducing elements in oxidizer}}{(-1)\ \Sigma \text{ oxidizing and reducing elements in fuel}} \qquad (1.2)$$

For α-Al_2O_3:

Metal nitrate: $Al(NO_3)_3$

Fuel: $(NH_2NH)_2CO$

$$\text{Oxidizer/fuel ratio} = \frac{(1Al \times -3) + (3N \times 0) + (9O \times 2)}{(-1)\ (1C \times -4) + (6H \times -1) + (4N \times 0) + (1O \times 2)} = \frac{15}{8} = 1.875$$

Hence, the stoichiometric aluminum nitrate:carbohydrazide molar ratio is 1:1.875. This ratio is required for the complete combustion of all materials.

The wet chemical method is used to achieve better mixing and uniformity of the final product. The wet chemical method of combustion synthesis was used in the current study in order to obtain a homogeneous, porous, crystalline powder for investigation. This work investigates the effects of combustion synthesis processing parameters on the physical properties of a simple oxide ceramic, α-alumina (α-Al_2O_3). Surface area, pore size, and residual carbon content were analyzed for the as-synthesized powders as a function of furnace temperature, fuel-to-oxidizer ratio, and precursor water content.

Alumina has been recognized for its abrasion resistance, chemical inertness, resistance to thermal shock, and mechanical strength at high temperatures[25]. It has been utilized for the production of metal-oxide-semiconductor (MOS) structures as gate oxides[26] among several other applications such as passivation layers[27], masks against impurities[28] and dielectric films in chemical sensors[29].

Recently, porous ceramics have found wide applications ranging from heterogeneous catalyst carriers and environmental filters for hot fuel gases and diesel engine emissions[30] to preforms for liquid metal infiltration in the production of ceramic-metal composites[31].

Several reports have focused on optimizing the combustion synthesis reaction in order that large surface areas may be obtained. Venkatachari *et al.*[32], in their investigation of combustion synthesized zirconia powders, found that mixtures of metal nitrates and oxalic dihydrazide ($C_2H_4N_2O_2$) fuel did not react at furnace temperatures of 250°C or less. They also found that as furnace temperature increased, the specific surface area increased. On the other hand, Hong *et.al.*[33], in their investigation of $Ca_{0.5}Sr_{0.5}Zr_4P_6O_{24}$ (CSZP) powders made by combustion synthesis, found that specific surface area decreased with increasing furnace temperature. This group also found that by increasing fuel content the specific surface area decreased due to the sintering effects of a long flame duration. In addition to furnace temperature effects, this group studied the effects of precursor water content. It was determined that specific surface area decreased with an increase in precursor water content. This was attributed to less heat being available for particle growth due to the heat of vaporization for water. The effect of processing parameters such as type of fuel, fuel/oxidizer ratio, furnace temperature, and precursor water content on the luminescent properties of yttrium aluminum garnet (YAG) phosphors has been studied[16]. It was shown that an increase in flame temperature resulted in an increase in luminous intensity of the as-synthesized phosphors. The objective of the present

study was to determine if physical properties, e.g. surface area, pore size, and residual carbon content could be affected via variation in furnace temperature, fuel/oxidizer ratio, and precursor water content. The combined effects of these processing parameters on the porosity of combustion synthesized powders has not been previously investigated, to the best of the authors knowledge.

2. EXPERIMENTAL PROCEDURE

2.1 Synthesis of Alumina

Aluminum Nitrate, $Al(NO_3)_3 \bullet 9H_2O$ (Sigma Chemical 99.999%) and carbohydrazide, $(NH_2NH)_2CO$ (Aldrich Chemical 98%) were mixed with deionized water in a 380 ml Coors porcelain dish. The two components dissolved, forming a clear viscous liquid. The mixture was stirred with a spatula, covered with a stainless-steel mesh and placed into a muffle furnace at 400, 500, or 600°C. Initially, the reactants underwent dehydration followed by decomposition. Upon further heating, the reactants ruptured into a flame. After ~10 seconds, the mixture was transformed into foamy, voluminous crystalline α-alumina powder that was then lightly crushed with a mortar and pestle to break up agglomerates.

In order to determine the effect of water content, deionized water was added until the aluminum nitrate and carbohydrazide were completely dissolved. This amount was typically between 0.668 and 0.698 ml of water per gram of metal nitrate. Fuel/oxidizer ratios of 1.2, 1.5, 1.7, 1.875, and 2.25 were used to study the effects of fuel/oxidizer ratio on surface area and average pore size. Table 1 lists the parameters evaluated in the production of porous α-alumina.

2.2 α-Alumina Characterization

X-ray diffraction (XRD) patterns of the combustion products were recorded using a Siemens D500 (Siemens Energy and Automation Analytical Instrumentation, Madison, WI) with $Cu_{K\alpha}$ radiation. Surface area was measured by the single point BET nitrogen adsorption method using a Micromeritics Flowsorb 2000 (Norcross, GA). The particle morphology and average pore size of the as-synthesized powders were studied using a scanning electron microscope (Stereo Scan 90, Cambridge Instruments, Thornwood, NY). A simultaneous thermal analyzer (STA-L85, Linseis, Princeton, NJ) was used to study the decomposition behavior of the precursor materials. The thermal analysis was conducted in flowing air (40 mL/min) using a heating rate of 20°C/ min to 480° then 5°C/min to 500°C and was held there for 3 minutes. Adiabatic flame temperature was estimated using Equation 1.1.

Average pore size was calculated from SEM micrographs using a line-intercept method. Ten lines were randomly drawn across a micrograph. The pores that were intersected by the lines were measured. The data were then analyzed to determine the averages and standard deviations of each sample. An elemental analyzer (240B, Perkin Elmer, Hartford, CT) was used to study the residual carbon content.

3. RESULTS AND DISCUSSION

3.1 Thermodynamics and Decomposition of the Combustion Reaction

Combustion synthesis reactions are typically conducted under non-adiabatic conditions therefore, the actual combustion temperature, T_c, is typically less than the maximum theoretical adiabatic combustion temperature, T_f. In this work, the adiabatic flame temperature for a stoichiometric reaction to form Al_2O_3, was estimated to be 2476°C using Hess' Law. However, in previous studies of combustion synthesis of α-alumina made with urea fuel, a flame temperature of 1600°C was measured using an optical pyrometer[4]. A flame temperature of 1825°C was measured for a chromium-doped yttrium aluminum garnet phosphor (YAG:Cr) produced by combustion synthesis using carbohydrazide[16].

The discrepancy between T_c and T_f is due to the losses associated with endothermic reactions during the formation of metal nitrate-fuel complexes; heat of vaporization of reactants; conduction and convection.

Differential thermal and thermogravimetric analyses (DTA/TGA) were performed for the aluminum nitrate, carbohydrazide, and the two reactants combined in the stoichiometric fuel/oxidizer ratio. The DTA/TGA for aluminum nitrate indicated two endothermic reactions, one at 97°C and the other 184°C, as shown in Figure 1. The first reaction was the evolution of adsorbed water from the atmosphere, and the second was the evolution of the waters of hydration from the as-received aluminum nitrate. Upon heating to 500°C the total mass loss was 94%.

Vetchinkina et al.[34], in their investigation of phase transformations in the thermal decomposition of aluminum nitrate, found that upon heating to 150°C the mass loss of the metal nitrate was 67% associated with decomposition of the original salt and the formation of amorphous α-alumina. From 200-500°C they found a marked weight loss of 86% of the original weight where the material remained amorphous. The α-alumina phase appeared in the 900-1000°C temperature range.

As shown in the DTA/TGA curves of Figure 2, the decomposition of carbohydrazide starts during the melting process at 159°C. Upon further heating, urazine, $C_2N_4H_4O_2$, is formed as an intermediate, with production of hydrazine. Hydrazine, N_2H_4, is the principal gaseous product in the decomposition of carbohydrazide[35]. Further decomposition produces CO_2. Beyond 15% conversion to CO_2 the reaction becomes autocatalytic as indicated by the exothermic peaks at 245°C and 325°C in Figure 2.

The decomposition of a stoichiometric aluminum nitrate-carbohydrazide mixture begins with the dehydration of adsorbed water and waters of hydration, followed by a decomposition of both materials and a sudden exothermic reaction at 235°C. The reaction continues to about 340°C, whereupon the fuel is turned completely into gases and the metal nitrate is transformed into the metal oxide, as shown in Figure 3:

3.2 Porosity Formation and Morphology

There can be four sources of porosity in combustion reaction products: (1) the initial porosity of the precursor mixture prior to reaction; (2) the change in volume that occurs between the reactants and products; (3) the rapid evolution of gases during the reaction; and (4) the diffusion of vacancies to produce micropores[31]. The as-synthesized powders in this work are macroporous (pore diameter, d_p > 50 nm). A SEM micrograph (Figure 4) of the as-synthesized powder reveals the bimodal porous nature of the combustion reaction.

If complete combustion is assumed, aluminum oxide is formed along with the liberation of the following gaseous products:

$$2\ AlN_3O_9\ (oxidizer) + 15/4\ CH_6N_4O\ (fuel) \rightarrow$$

$$Al_2O_3\ (s) + 45/4\ H_2O\ (g) + 15/4\ CO_2\ (g) + 21/2\ N_2\ (g)$$

However, the amount of fuel needed to react completely with the oxidizer depends on the final oxidation state of nitrogen, carbon, and hydrogen[36]. There is evidence that nitrogen can have a valence of +2 (as NO), +2x (as NO_x), or +4 (as NO_2) after the combustion reaction[37]. Therefore, calculations of the stoichiometric composition are based on the assumption that the nitrogen species in the product has a valence of 0. That may not always be the case, making the calculation of stoichiometric amounts difficult. There will be further investigation in order to determine the exact valences of all products.

3.3 Effect of Processing Parameters

(A) *Effect of Furnace Temperature*:

XRD patterns confirmed single-phase α-alumina for all variations in furnace temperature (Figure 5).

As furnace temperature increased, average pore size markedly decreased from 1.2 to 0.2 μm. Figure 6 shows the effect of furnace temperature on average pore size of the as-synthesized powders. Furnace temperature was not found to have a significant effect on specific surface area in this study, i.e. surface areas were 20, 16, and 17 m^2/g for furnace temperatures of 400, 500, and 600°C.

Furnace temperature also effected the residual carbon content in as-synthesized powders made from dry and aqueous precursors. As furnace temperature increased, the amount of residual carbon decreased. The faster heating rate of the precursor at progressively higher furnace temperatures can account for this difference.

(B) *Effect of Fuel/Oxidizer Ratio:*

XRD patterns for the fuel lean (fuel/oxidizer ratio 1.5 and 1.7), stoichiometric and fuel rich reactions, dry and dissolved, showed phase pure α-alumina. XRD patterns for the fuel lean (fuel/oxidizer ratio 1.2) reactions, dry and dissolved, showed amorphous products. Traces of crystalline α-alumina and dehydrated aluminum nitrates were found (Figure 7). This is possibly due to the flame temperature being too low for complete oxide formation because of the

scarcity of fuel. These findings agree with what Venkatachari *et al.*[32] have discovered regarding fuel lean reactions.

Carefully-controlled combustion synthesis can yield nano-crystalline powder with high specific surface areas. The BET surface area of the as-synthesized powders fell into the range of 6 to 58 m^2/g. These surface area values agree with those obtained for metal zirconate powders made by metal nitrate-carbohydrazide combustion synthesis[14]. In this work, surface area was found to be strongly influenced by fuel/oxidizer ratio. Powders with maximum surface area were obtained for the 1.2 fuel lean reactions and the lowest surface area was obtained for the 2.25 fuel rich reaction (Figure 8). This trend agrees with what Hong *et al.*[33] have found regarding surface area as a function of increased fuel content. Namely, that additional fuel may cause sintering, due to longer flame duration. This explains the decrease in surface area of the powders at higher fuel/oxidizer ratios.

By increasing the fuel/oxidizer ratio, average pore size also decreases due to sintering effects and a longer flame duration as a result of additional fuel. This is illustrated in Figure 9.

(C) *Effect of Precursor Water Content:*

The elemental analysis data indicated that more residual carbon is present in as-synthesized powders made from dry precursors than in powders made from aqueous precursors. As previously mentioned, dry carbohydrazide decomposes into urazine and N_2H_4 when heated. However, in aqueous solution, H_2O may be inserted into the C-N bond of carbohydrazide, resulting in CO_2 and

N_2H_4 being the most favorable by-products[38]. Hence, more carbon remains after combustion of dry precursors due to the formation of carbonaceous reaction intermediates. This is the case at 1.5 and 1.7 fuel/oxidizer ratios where the aqueous reactions produced less carbon than the dry reactions. The 1.875 and 2.25 fuel/oxidizer ratios are currently under investigation.

4. CONCLUSIONS

A low-temperature initiated exothermic redox reaction involving a metal nitrate-carbohydrazide mixture, which was employed in the synthesis of crystalline, macroporous aluminum oxide powders has been described. It has been shown that furnace temperature, fuel/oxidizer ratio, and precursor water content can be tailored to produce different physical properties. Studies showed that increasing furnace temperature did not have a significant effect on specific surface area of the product powders; however average pore size markedly decreased. Surface area and average pore size was found to decrease with increasing fuel/oxidizer ratio. Elemental analysis showed decreasing residual carbon content with increased temperature and precursor water content. Therefore, high precursor water content combined with a low furnace temperature and a fuel lean reaction yielded the purest product powder with the largest BET surface area and the largest average pore size. The dissolved reaction with a higher furnace temperature (600°C) and a fuel rich reaction created powders with the smallest BET surface area and the smallest average pore size.

References

1. A. G. Merzhanov and I. P. Borovinskaya, Dokl. Chem. (Engl. Transl.), **204** [2] 429-432 (1972).
2. W-C. Lee, C-L. Tu, C-Y. Weng, and S-L. Chung, J. Mater. Res., **10** [3] 774-778 (1995).
3. J. J. Moore and H. J. Feng, Prog. Mat. Sci., **39**, 275-316 (1995).
4. J. J. Kingsley and K. C. Patil, Mat. Lett., **6** [11,12] 427-432 (1988).
5. J. J. Kingsley, N. Manickam, and K. C. Patil, Bull. Mater. Sci., **13** [22] 179-189 (1990).
6. P. Ravindranathan, S. Komarneni, and R. Roy, J. Mater. Sci. Lett., **12**, 369-371 (1993).
7. J. J. Kingsley and K. C. Patil, Ceramic Transactions, Ceramic Powder Science II, eds. G. L. Messing, S. Hirano, and H. Hausner, **12**, 217-224 (1992)
8. N. Balagopal, K. G. K. Warrier, and A. D. Damodaran, J. Mater. Sci. Lett., **10**, 1116-1118 (1991).
9. J. J. Kingsley and L. R. Pederson, Mat. Res. Soc. Symp. Proc., **296**, 361-366 (1993).
10. L. A. Chick, G. D. Maupin, and L. R. Pederson, Nanostructured Materials, **4** [5] 603-615 (1994).
11. L. A. Chick, L. R. Pederson, G. D. Maupin, J. L. Bates, L. E. Thomas, and G. J. Exarhos, Mater. Lett., **10** [1,2] 6-12 (1990).

12. N. J. Hess, G. D. Maupin, L. A. Chick, D. S. Sunberg, D. E. McCready, and T. R. Armstrong, J. Mater. Sci., **29** [7] 1873-1878 (1994).

13. L. R. Pederson, G. D. Maupin, W. J. Weber, D. J. McCready, and R. W. Stephens, Mater. Lett., **10** [9] 437-443 (1991).

14. N. Dhas and K. C. Patil, J. Mater. Chem., **3** [12] 1289-1294 (1993).

15. J. J. Kingsley, K. Suresh, and K. C. Patil, J. Sol. Stat. Chem., **87**, 435-442 (1990).

16. L. E. Shea, J. McKittrick, and O.A. Lopez, *J. Am. Ceram. Soc.* **79** [12] 3257-3265 (1996).

17. L. E. Shea, J. McKittrick, and M. L. F. Phillips, *Mat. Res. Soc. Symp. Proc.* Flat Panel Display Materials II, **424**, 409-414 (1996).

18. E. J. Bosze, G. A. Hirata, J. McKittrick, and L. E. Shea, *J. of SID*, in press.

19. G.Y. Onoda, Jr. and L.L. Hench, *Ceramic Processing Before Firing* (Wiley, New York, 1978)

20. H. Schumann, N. Conrad, and R. Schradev, *Chem. Abstr.* **83**, 197340d (1975)

21. J. G. M. De Lau, *Amer. Ceram Soc. Bull* **49** [6] 572 (1970).

22. D. R. Messier and G. E. Gazza, *ibid.* **51** [9] 692 (1972).

23. A. Sen and D. Chakravorty, in "Advances in Solid State Chemistry"; pp.159. Edited by C. N. R. Rao. INSA, New Delhi, 1986.

24. B. Jower, J. Juhasz, and G. Szabo Zoltan, *Chem, Abstr.* **100,** 28804x (1984).

25. A. K. Dua, V. C. George, and R. P. Afarwala, *Thin Solid Films*, **165,** 163

(1988).

26. J. Saraie and S. Ngan, *Jpn. J. Appl. Phys. Part I*, **29**, 1877 (1990).

27. J. Tsujide, S. Nakamura, and Y. Ikushima, *J. Electrochem. Soc.* **117**, 703 (1970).

28. B.E. Deal and J.M. Early, *J. Electrochem. Soc.* **126**, 20C (1979).

29. C. Nylander, M. Argarth, and O. Sevensson, *J. Appl. Phys.*, **56**, 177 (1984).

30. W. Zhou, W. B. Hu, and D. Zhang, *J. Mate. Sci.* **34**, 4469-4473 (1999).

31. J. J. Moore and H. J. Feng, *Prog. in Mate. Sci.* **39**, 243-273 (1995).

32. K. R. Venkatachari, Dai Huang, S. P. Ostrander, W. A. Schulze, and G. C. Stangle, *J. Mater. Res.*, **10** [3] 748 (1995).

33. C. S. Hong, P. Ravindranthan, D. K. Agrawal, and R. Roy, *J. Mater. Res.*, **9** [9] 2398 (1994).

34. T. N. Vetchinkina, A. I. Ezhov, and Yu. A. Lainer, Translated from *Zhurnal Neorganicheskoi Chimii*, **31**, 296-300 (1986).

35. E. Nachbaur, E. Baumgartner, and J. Schober, 2nd European Symposium on Thermal Analysis, 417-421 (1981).

36. Y. Zhang and G.C. Stangle, J. Mater. Res., **9** [8] (Aug 1994)

37. D.C. Hitchcock, R. P. Rusin, and D. L. Johnson. *J. Am. Ceram. Soc.* **74**, 2165-2169 (1991).

38. J. W. Schoppelrei and T.B. Brill, *J. Phys. Chem.*, **101**, 2298-2303 (1997)

Acknowledgements: This work was supported by Sandia National Laboratories. Sandia is a multiprogram laboratory operated by Sandia Corporation, a Lockheed Martin Company, for the United States Department of Energy under contract No. DE-

AC04-94AL85000. The authors express their thanks to Robert Derby for providing SEM analysis and Ernie Montoya for BET analysis.

Table 1. Compositions used in Combustion Synthesis Reactions

Fuel/Oxidizer Molar Ratio	Precursor Water Content	400°C	500°C	600°C
1.2	Dry	X	X	X
	Dissolved	X	X	X
1.5	Dry	X	X	X
	Dissolved	X	X	X
1.7	Dry	X	X	X
	Dissolved	X	X	X
1.875	Dry	X	X	X
2.25	Dry	X	X	X

LIST OF FIGURES

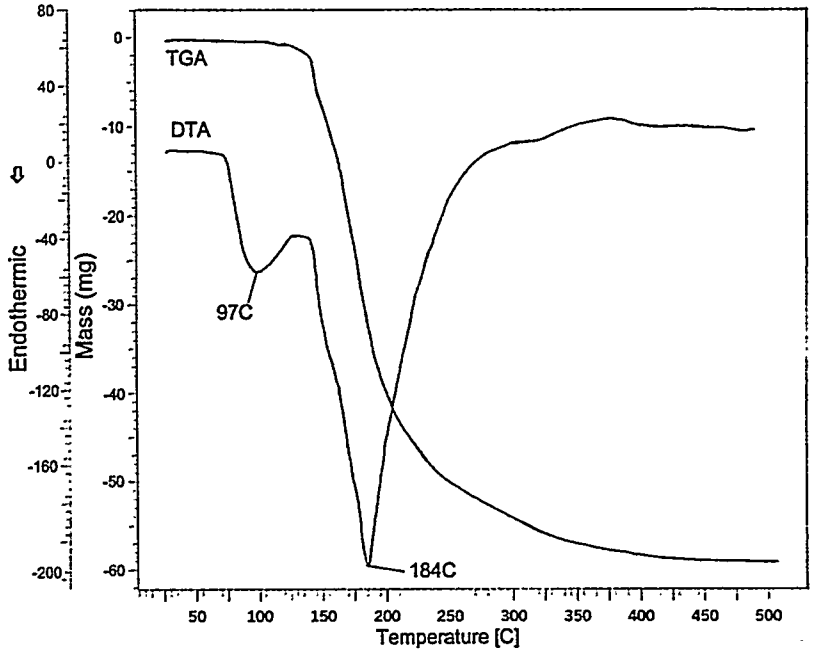

Figure 1: Differential Thermal Analysis (DTA) and Thermogravimetric Analysis (TGA) patterns for aluminum nitrate.

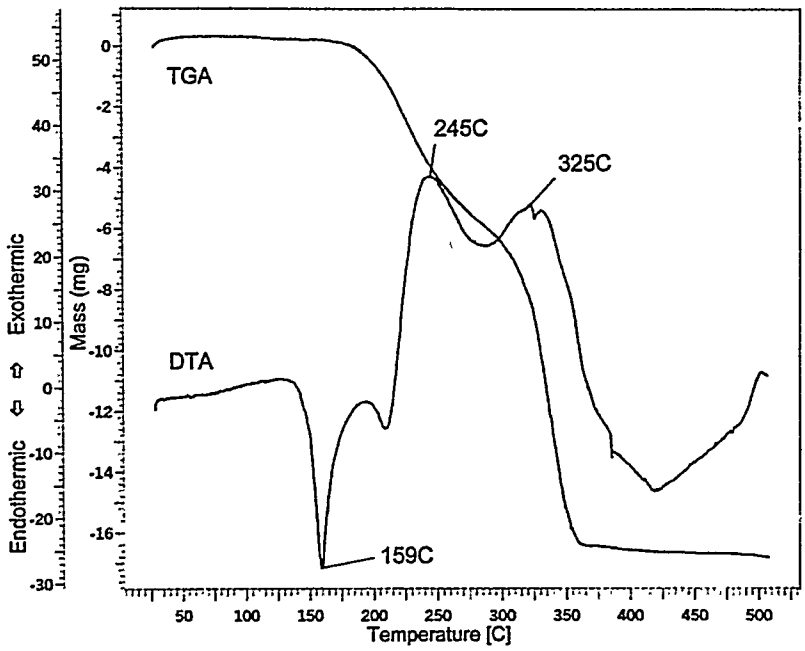

Figure 2: DTA/TG analysis patterns for carbohydrazide.

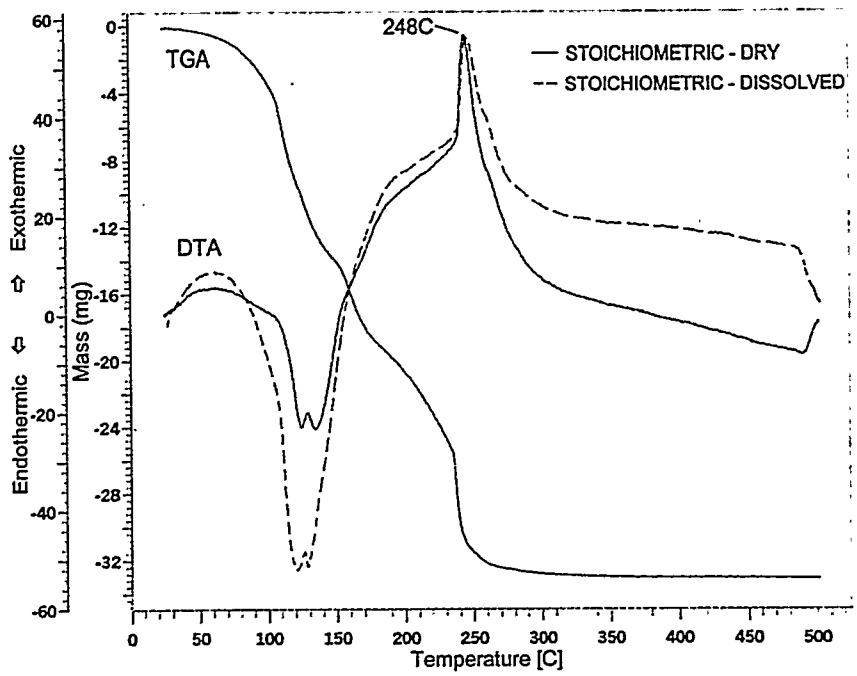

Figure 3: DT/TGA patterns of aluminum nitrate-carbohydrazide dry and dissolved stoichiometric mixtures. TGA pattern is typical of dry and dissolved reaction.

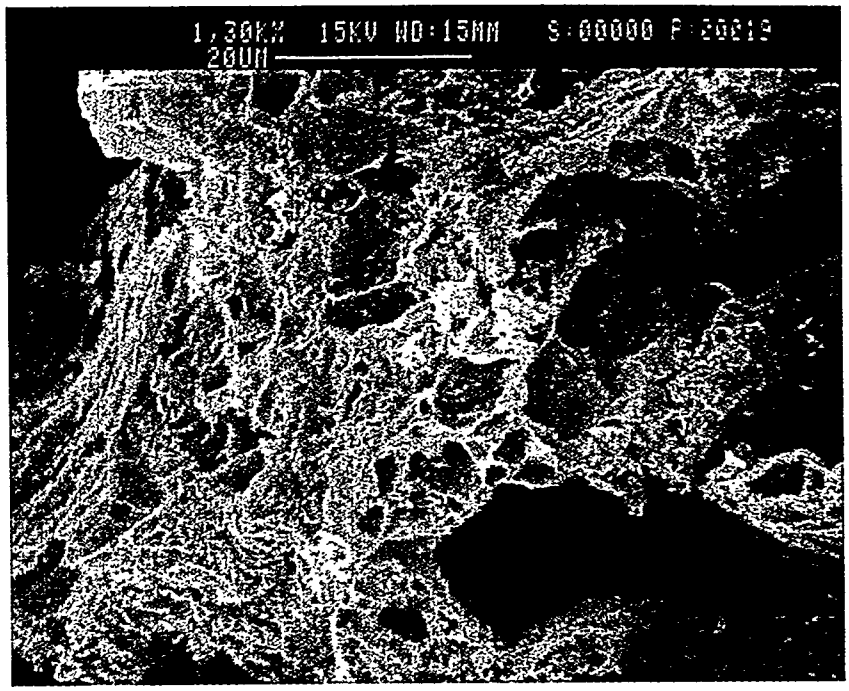

Figure 4: SEM micrograph of α-alumina powder made by combustion synthesis.

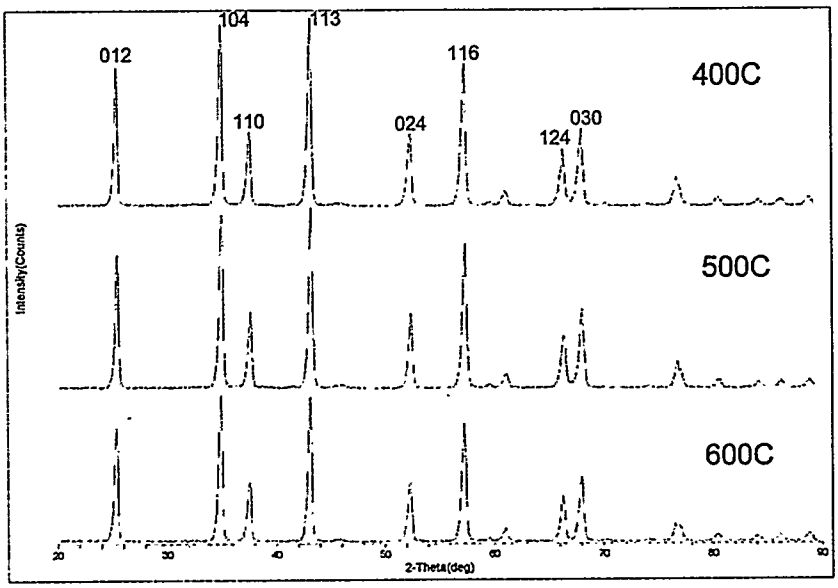

Figure 5: X-ray diffraction data showing single phase α-alumina for the 400°C, 500°C and 600°C fuel lean (fuel/oxidizer ratio = 1.5) reactions.

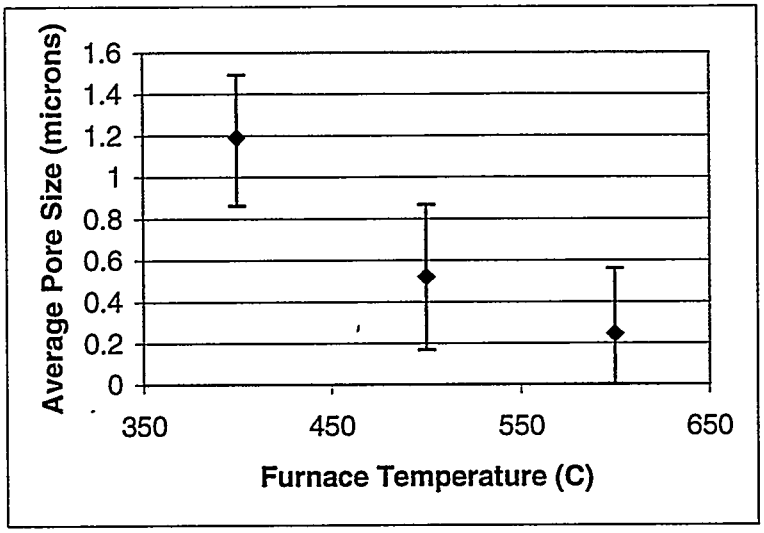

Figure 6: Average pore size as a function of furnace temperature for the fuel lean reaction. Average pore size in microns decreases as a function of furnace temperature for the fuel lean (fuel/oxidizer ratio = 1.5) reaction (95% confidence interval shown).

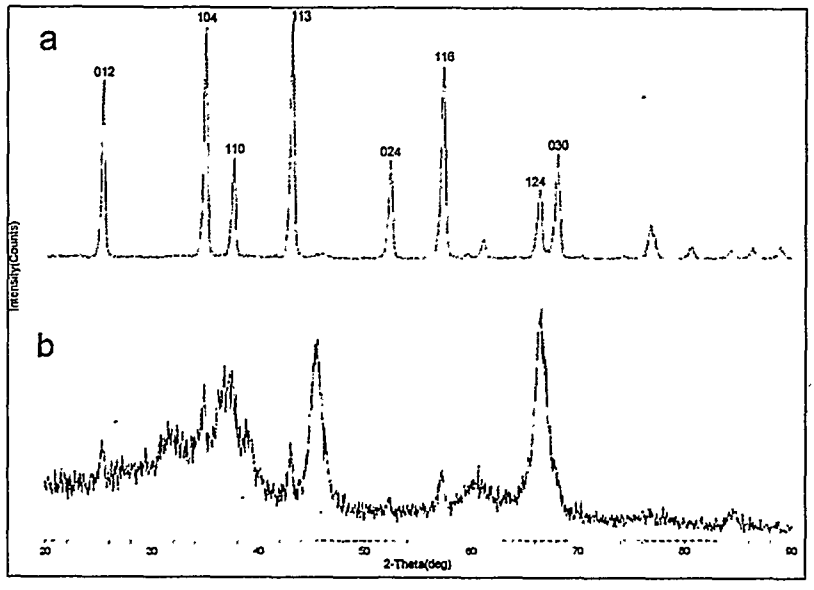

Figure 7: Phase pure and amorphous α-alumina XRD patterns. (a) phase pure α-alumina stoichiometric reaction at 600°C (b) amorphous α-alumina fuel lean reaction with organic residuals at 600°C

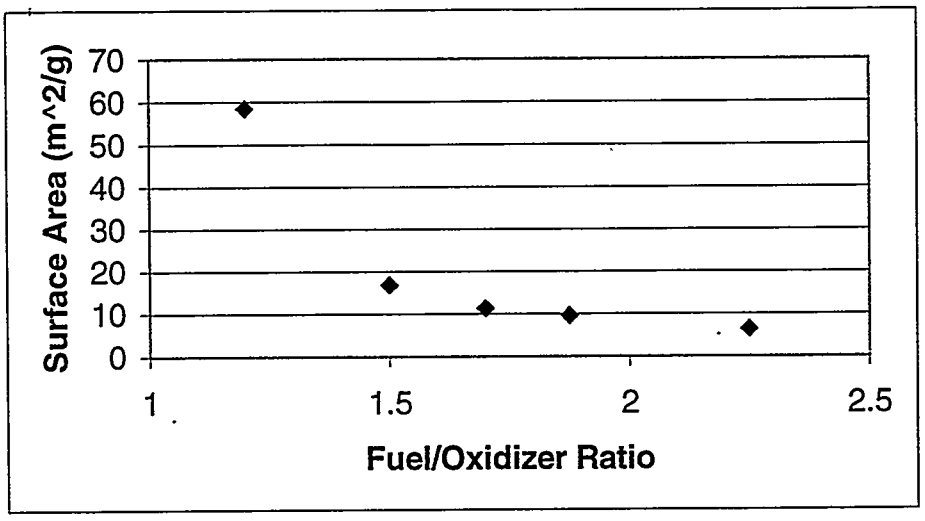

Figure 8: BET surface area as a function of fuel/oxidizer ratio for 500°C.

BET surface area decreases as a function of fuel/oxidizer ratio for a furnace temperature of 500°C.

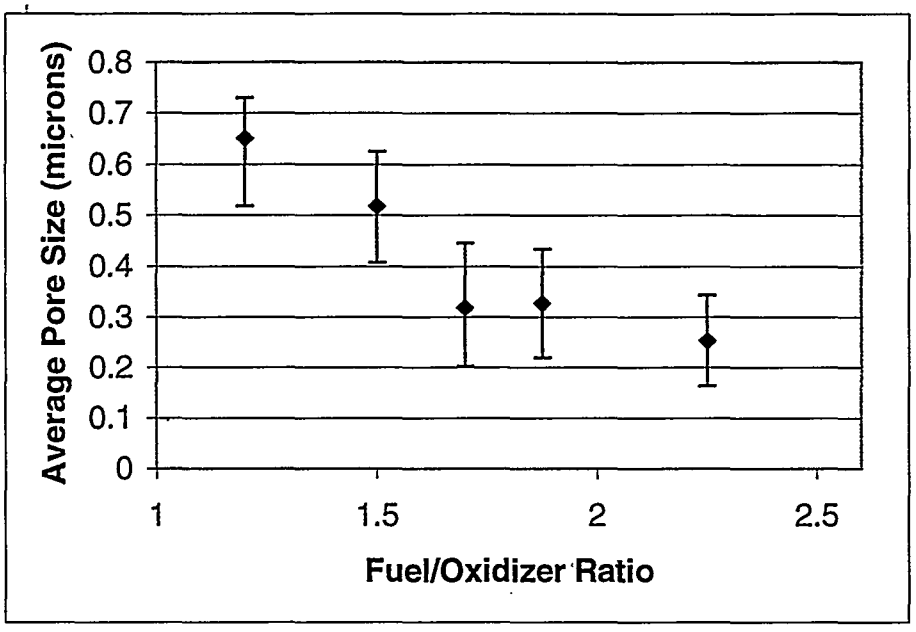

Figure 9: Average pore size as a function of fuel/oxidizer ratio for 500°C. Average pore size in microns decreases as the fuel/oxidizer ratio increases (95% confidence interval).

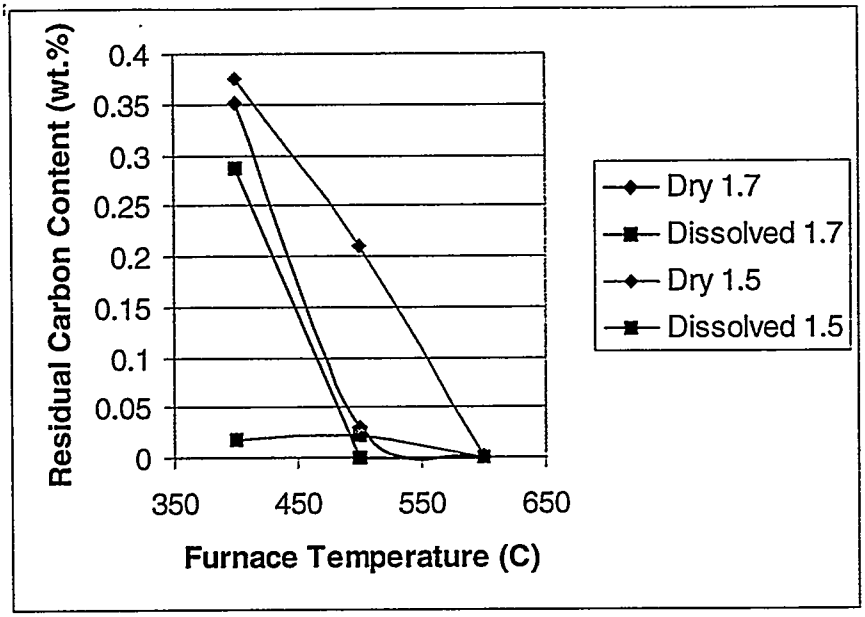

Figure 10: Residual carbon content as a function of furnace temperature for the fuel lean reactions (fuel/oxidizer ratio 1.5 and 1.7).